Image Matching with Characteristic Information of Gray Value and Interest Points

Dong-Cheon Lee, Jae-Hong Yom, Sun-Ok Choi, and Su-Jeong Kim
Dept. of Geoinformation Engineering / Research Institute of Geoinformatics & Geophysics
Sejong University
98 Gunja-Dong, Gwangin-Gu, Seoul, 143-747 Korea
dclee@sejong.ac.kr

Abstract: Image matching is fundamental process to identify conjugate points on the stereo images. However, standard methods or general solutions for matching problem have not been found yet, in spite of long history. Quality of the matching basically depends on uniqueness of the matching entity and robustness of the algorithm. In this study, conjugate points were extracted by implementing interest operator, then area based matching method was applied to the topographical characteristics of the gray value as the matching entities. The matching entities were utilized based on the concept of the intrinsic image.
Keywords: Image matching, Digital image, Interest operator, Intrinsic image.

1. Introduction

Image matching is an essential task for orientations in photogrammetry and object recognition in computer vision. The ultimate goal of the image matching is to achieve reliable identification of the corresponding features efficiently and automatically without human intervention [1]. In this study, Harris interest operator was used to select distinct conjugate points in the aerial stereo pair images. As for the matching entities, not only gray value itself but also topographical characteristics of the gray value were utilized. Then, cross-correlation matching method was followed. The topographical characteristics in this paper are adopted from concept of the intrinsic image. Intrinsic images that consist of illumination, surface orientation, reflectance and depth have more explicit and meaningful information than images represented by gray value only. Slope, aspect and reflectance derived from gray values were used as matching entities. Gray value, slope and aspect, and reflectance may correspond to illumination, surface orientation, and reflectance in the intrinsic image, respectively. Topographical characteristics of the gray values do not directly refer to the physical surface topography. Information from the characteristics may be used supplementary or additional

2. Extraction of Interest Points

Interest points are distinct features that have great possibility to be selected as conjugate points because detection and identification are easy with well-defined. There are important requirements for interest points: (a) View-point invariant, (b) Rotation invariant, (c) Sufficient information in the neighborhood of the target pixels, and (d) Isolated feature [2, 3, 4]. The motivation for determining interest points is to find image patches of sufficient and reliable information so that matching has a higher potential to be successful. In this study, interest points - especially corner points - were extracted by using Harris operator that based on the partial derivatives of the gray value [5].

Matrix M is computed within a certain window over the entire image as:

$$M = \begin{bmatrix} \left(\frac{\partial g(i,j)}{\partial x}\right)^2 & \left(\frac{\partial g(i,j)}{\partial x}\right)\left(\frac{\partial g(i,j)}{\partial y}\right) \\ \left(\frac{\partial g(i,j)}{\partial x}\right)\left(\frac{\partial g(i,j)}{\partial y}\right) & \left(\frac{\partial g(i,j)}{\partial x}\right)^2 \end{bmatrix} \quad (1)$$

where $g(i,j)$ is gray value of the image, $\partial g/\partial x$ and $\partial g/\partial y$ are partial derivatives with respect to x- and y-direction, respectively. The response function of the interest point is given by:

$$R = det\ (M) - k \cdot [trace\ (M)]^2 \quad (2)$$

where k is a parameter based on the empirical value, usually between 0.04 and 0.06. Interest points are determined as global maximum of the response function over the entire image, *i.e.,* if $g(i,j) \geq T \cdot R_{max}$ then pixels at (i,j) are assigned as interest points with R_{max} is a maximum response. In practice, often more points are extracted around a certain feature in the same area. Therefore, refinement is required to determine the unique point. In this study, weighted average was implied to locate refined interest points:

$$x = \frac{\sum R_{ij} x_i}{\sum R_{ij}}, \quad y = \frac{\sum R_{ij} y_i}{\sum R_{ij}} \quad (3)$$

Other options for refinement are to compute centroid or local maximum around extracted interest points. Weight average and centroid provide sub-pixel location of the points. Window size = 3 x 3, $k = 0.04$ (suggested by Harris), and $T = 0.1$ were used in this study.

3. Intrinsic Image and Topographical Characteristics of Gray Value

A digital image is considered as a matrix whose row and column indices identify location in the image and the corresponding element identifies the gray value at the point, *i.e.,* pixel. Fig. 1 represents a digital image and 3D representation of the gray value distribution. An image is formed by recording reflected EMR (electro-magnetic radiation) energy from the Earth and object surface. Therefore, the interaction of EMR with the surface is most important factor in the image formation process.

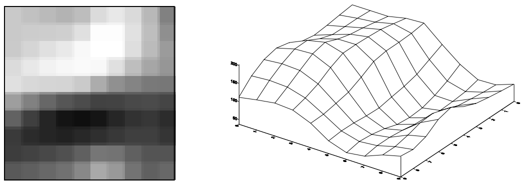

(a) Gray values. (b) 3D view of the gray value distribution.
Fig. 1. Topographic representation of gray values.

1) Intrinsic Image

The most dominant factors that have influence on the interaction of EMR with the surface are illumination, surface orientation, reflectance and depth. However, gray values of the image are mixed result of all factors in image formation. Therefore, an intrinsic image provides more useful information about geometric and physical characteristics of the scene than gray value. Therefore, application of the intrinsic information is helpful to solve the ill-posed nature of the image matching, surface reconstruction, object recognition, *etc*.

2) Topographical Characteristics of Gray Value

Gray value is not directly related with topography of the actual surface. In other words, the bigger gray value does not depict the higher elevation of the surface, and *vice versa*. However, the topography of the gray value, for example, slope, aspect and reflectance may provide additional or supplementary information.

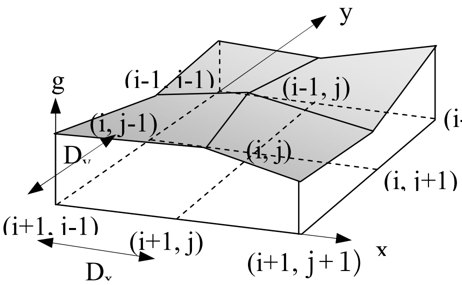

Fig. 2. Gray value represented in 3D space.

Gray value is treated as elevation in DEM (digital elevation model) (Fig. 2). Then, following characteristics are computed to analyze topographic characteristics of the gray value [6]:

- Slope:

$$S = \left[\sqrt{\Delta g_x^{\,2} + \Delta g_x^{\,2}}\right] / 2 \qquad (4)$$

where Δg_x , Δg_y are gray value differences in x- and y-direction, respectively.

- Aspect:

$$\alpha = tan^{-1}(\Delta g_x / \Delta g_y) \qquad (5)$$

- Reflectance:

$$R = \frac{(X_s S_x + Y_s S_Y + r)}{\sqrt{(1 + S_x^{\,2} + S_Y^{\,2})(1 + X_x^{\,2} + Y_s^{\,2})}} \qquad (6)$$

where $X_s = r \cos E_s \cos A_s$, $Y_s = r \cos E_s \sin A_s$, $Z_s = -r$. E_s, A_s, S_x and S_y are solar elevation angle, solar azimuth, x- and y-direction slope, respectively. Slope and aspect provide the information about surface orientation.

It is noticed that the reflectance was computed by applying shading or shaded relief algorithm [7]. Above characteristics (*i.e.,* slope, aspect and reflectance) and gray value itself were used as matching entities. Fig.3 shows test images (pixel size:28μmx28μm). Fig.4 and Fig. 5 show surface orientation and shaded relief derived from gray value of the stereo pair, respectively.

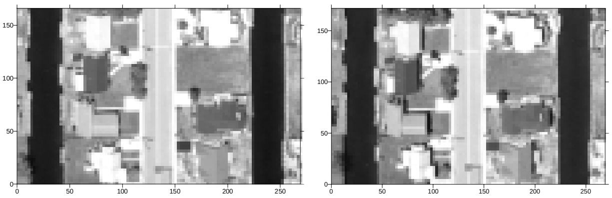

(a) Left image. (b) Right image.
Fig. 3. Patches of stereo pair of aerial images.

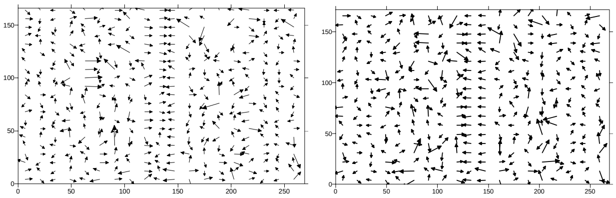

(a) Left image. (b) Right image.
Fig. 4. Surface orientation derived from slope and aspect of gray value.

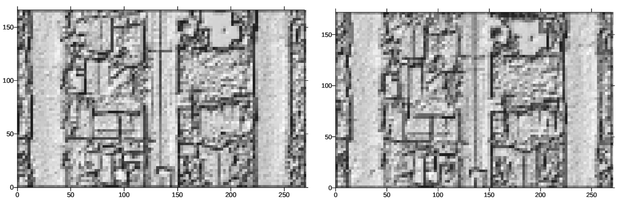

(a) Left image. (b) Right image.
Fig. 5. Reflectance derived from gray value.

4. Image Matching

Cross-correlation matching method was implemented to determine the conjugate points. The important issues in image matching, especially for the area-based matching, are location and size of both template and search region, and acceptance criteria [4]. In this study, the locations of the template and search region were selected based on the extracted interest points. The cross- correlation coefficient is computed by:

$$\rho = \frac{\sigma_{LR}}{\sigma_L \sigma_R} \tag{7}$$

where σ_{LR} is covariance of left and right image patches, σ_L, and σ_R are standard deviation of left (*i.e.,* template) and right image patches (*i.e,* matching window), respectively. The template was centered on the interest points on the left image then, the matching windows were centered on the interest points (Fig. 6). The cross-correlation coefficients were computed with matching entities within the search region. In order to find the matched conjugate points, the cross-correlation coefficients were analyzed (Table 1 and Fig. 7).

.

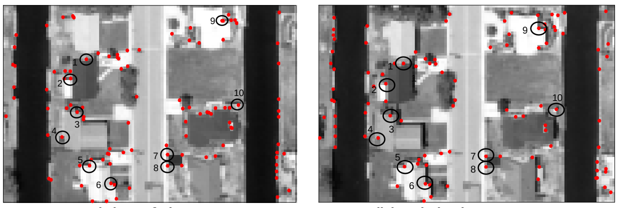

(a) Left image. (b) Right image.

Fig. 6. Interest points.

Table1. Summary of results. (I: interest pt, C: conjugate pt)

Point No. Coords.	CCC	Gray value	Slope	Aspect	Reflectance
1 I: (77,121)	ρ_{max} (coord.)	0.91 (76,121)	0.95 (76,121)	0.98 (83,121)	0.91 (76,121)
C: (76,121)	ρ_c	**0.64**	**0.45**	**0.53**	**0.91**
2 I: (61,103)	ρ_{max}	0.88 (66,101)	0.95 (60,105)	0.98 (61,104)	0.93 (61,104)
C: (61,104)	ρ_c	**0.83**	**0.43**	**0.98**	**0.93**
3 I: (65,75)	ρ_{max}	0.87 (65 ,75)	0.71 (65,75)	0.94 (62 ,73)	0.95 (65,76)
C: (65,76)	ρ_c	**0.86**	**0.71**	**0.92**	**0.95**
4 I: (54,56)	ρ_{max}	0.82 (54,56)	0.83 (57, 52)	0.99 (54,56)	0.93 (54,56)
C: (54,56)	ρ_c	**0.82**	**-0.07**	**0.99**	**0.93**
5 I: (78,31)	ρ_{max}	0.98 (78,31)	0.70 (78,31)	0.97 (78,31)	0.83 (78,31)
C: (78,31)	ρ_c	**0.98**	**0.70**	**0.64**	**0.83**
6 I: (97,16)	ρ_{max}	0.94 (97,16)	0.76 (101,15)	0.94 (98,17)	0.95 (97,16)
C: (97,16)	ρ_c	**0.94**	**0.35**	**0.23**	**0.95**
7 I: (152,40)	ρ_{max}	0.99 (152 ,40)	0.97 (152,40)	0.98 (148,38)	0.99 (152,40)
C: (152,40)	ρ_c	**0.99**	**0.97**	**0.97**	**0.99**
8 I: (152,31)	ρ_{max}	0.99 (152,30)	0.97 (152,30)	0.99 (152,30)	0.99 (152,30)
C: (152,30)	ρ_c	**0.99**	**0.97**	**0.99**	**0.99**
9 I: (200,152)	ρ_{max}	0.96 (199,152)	0.97 (199,156)	0.87 (199,152)	0.85 (199,152)
C: (199,152)	ρ_c	**0.96**	**0.93**	**0.87**	**0.85**
10 I: (216,81)	ρ_{max}	0.89 (215,81)	0.80 (218,79)	0.96 (216,81)	0.94 (216,81)
C: (216,81)	ρ_c	**0.83**	**0.72**	**0.96**	**0.94**

(*Note:* ρ_{max} denotes maximum cross-correlation coefficient. ρ_c denotes cross-correlation on actual conjugate point.)

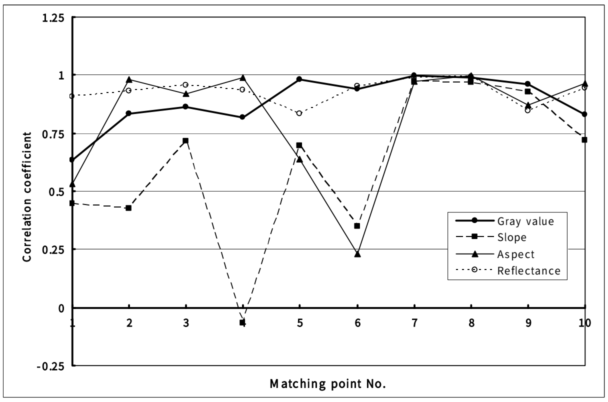

Fig. 7. Cross-correlation on conjugate points.

5. Conclusions

Matching on interest points provided high correlation coefficients because interest points are distinct and unique features. Overall correlation coefficient was higher than 0.8. Therefore, matching quality and reliability increases by utilizing interest operator.

The characteristic information derived from gray value has great potential to be matching entity together with gray value. The optimal solution in matching problem could be obtained by utilizing appropriate matching entities. Therefore, it is suggested that to derive reasonable matching entities and algorithm to achieve robust matching.

Acknowledgement

This study was supported by National Research Lab (Ministry of Science & Technology, Grant No. M10302000063-03J0000-03210). The aerial images were provided by ISPRS Commission III.

References

[1] Heipke, C., 1997. Automatic Image Orientation in Special Issue, *ISPRS Journal of Photogrammetry and Remote Sensing*, 52(3).

[2] Konrad, J. and Z. Lan, 2000. Density Disparity Estimation from Feature Correspondences, *Proc. IS&T/SPIE Symposium on Electronic Imaging Seteroscopic Displays and Virtual Reality System,* San Jose, CA, USA, pp.23-28.

[3] Mikhail, E., J. Bethel, and J. McGlone, 2001. Introduction to Modern Photogrammetry, John Wiley & Sons, New York, NY, USA.

[4] Schenk, T., 1999. Digital Photogrammetry, TerraScience, Columbus, OH, USA.

[5] Harris, C. and M. Stephens, 1988. A Combined Corner and Edge Detector", *4th Alvey Vision Conference*, pp.147-151, 1988.

[6] Burrough, P., 1988. Principles of Geographical Information Systems for Land Resources Assessment, Oxford University Press, Oxford, UK.

[7] Horn, B., 1986. Robot Vision, The MIT Press, New York, NY, USA.